Computer Aided Diagnostic System for Detection and Classification of a Brain Tumor through MRI Using Level Set Based Segmentation Technique and ANN Classifier

Atanu K Samanta, Asim Ali Khan

Abstract—Due to the acquisition of huge amounts of brain tumor magnetic resonance images (MRI) in clinics, it is very difficult for radiologists to manually interpret and segment these images within a reasonable span of time. Computer-aided diagnosis (CAD) systems can enhance the diagnostic capabilities of radiologists and reduce the time required for accurate diagnosis. An intelligent computer-aided technique for automatic detection of a brain tumor through MRI is presented in this paper. The technique uses the following computational methods; the Level Set for segmentation of a brain tumor from other brain parts, extraction of features from this segmented tumor portion using gray level co-occurrence Matrix (GLCM), and the Artificial Neural Network (ANN) to classify brain tumor images according to their respective types. The entire work is carried out on 50 images having five types of brain tumor. The overall classification accuracy using this method is found to be 98% which is significantly good.

Keywords—Artificial neural network, ANN, brain tumor, computer-aided diagnostic, CAD system, gray-level co-occurrence matrix, GLCM, level set method, tumor segmentation.

I. INTRODUCTION

A brain tumor is an abnormal growth of tissue in the brain or central spine that can hamper proper brain function. The masses grow rapidly in an uncontrolled way. A primary brain tumor starts from cells in the brain. Secondary tumors are mainly generated from another part of the body. Secondary brain tumors are actually composed of cancer cells from somewhere else in the body that have been metastasized, or spread already to the brain [1]. A central nervous system tumor contributes a distinct group of diseases that vary from benign, slow-growing lesion to aggressive malignancies that can cause death. Each of these tumors has unique pathological, radiological, and anatomic characteristics. Benign tumors grow gradually and do not spread widely. Malignant tumors grow more quickly compared to benign tumors and can spread to surrounding tissues. Once a brain tumor is clinically suspected, radiological evaluation is required to determine the location, the extent of the tumor and its relationship to the surrounding structures [2]. MRI is the most appreciated modality of brain tumor imaging for proper diagnosis of patients who have a brain tumor. Its multiplane capability,

Atanu K Samanta and Asim Ali Khan are with the Sant Longowal Institute of Engineering and Technology, EIE Department, Longowal, Punjab, India (e-mail: samanta.atanu123@gmail.com, asimsliet@gmail.com).

superior contrast resolution and flexible protocols allow it to diagnose the tumor location and extent [2]. Studies on CAD systems and technology show that CAD can help to improve the diagnostic accuracy of radiologists, ease the burden of increasing workload, as well as improve inter- and intra-reader variability [3]. The standard protocol most commonly used includes: spin-echo T1-weighted image (T1WI), proton density-weighted image (PDWI), T2-weighted image (T2WI), and T1WI after the administration of a paramagnetic agent. Most brain tumors have prolonged T1 and T2 relaxation times and appear hypo-intense relative to normal brain on T1WI and hyper-intense on T2WI. On PDWI, the tumors show intermediate hyper-intensity [4]. The CAD systems are designed to provide a second opinion for radiologists using various machine learning techniques. The heterogeneous nature of different types of tumor and the presence of edema around the tumor makes the segmentation process a bit difficult and complex. Therefore, the main focus of this present work is to develop an efficient and accurate brain tumor detection system.

II. RELATED WORK

The high resolution MR image of the brain contains a considerable amount of skull, scalp, eyeballs, fat, and muscle, etc. To improve the diagnostic accuracy, these non-brain parts of the image are to be removed before final segmentation. Smith [5] developed an automated, fast and robust method for segmenting MR head scans into brain and non-brain parts. Somasundaram [6] proposed two unsupervised and knowledge based methods to extract brain parts automatically using region labeling and morphological operations. A hybrid level set based active contour neighborhood model for brain extraction proposed by Jiang [7], uses a non-linear speed function.

Brain tumor segmentation methods can be classified into three main categories including manual, semi-automatic, and fully automatic segmentations based on the degree of required human interaction. In fully automatic brain tumor segmentation, the computer determines the segmentation of brain tumor without any human interaction. Whereas in semiautomatic brain tumor segmentation, the human presence is often needed to initialize the method by selecting various parameters of certain algorithm, to check the segmentation

accuracy and feedback the result, or in some cases to manually correct the segmentation result.

The brain tumor segmentation requires an objective measure that can be used to define the homogeneity of each tissue. There exists two ways of obtaining the objective measures: the unsupervised and supervised segmentation methods. The difference between them is that unsupervised methods do not make use of manually labeled training data. In the unsupervised segmentation, the number of classes is automatically specified by an algorithm that groups numerically similar pixels [8].

In general, the segmentation technique is used to partition a processed image based on changes in intensity values, edges and corners or to partition an image into its consequent regions that are similar with respect to a certain set of predefined criteria. At present, techniques such as thresholding [9], region growing [10], [11], active contour and shape based models [4], [12], [13], knowledge based approaches [14], [15], machine learning based such as clustering [16]-[18] have been used for image segmentation.

Optimal global thresholding using Otsu's Method is used to perform histogram shape-based image thresholding automatically or to convert the gray-scale image to a binary image [19]. The algorithm presumes that the image to be thresholded contains only two classes of pixels or bi-modal histogram (e.g. foreground and background) and then calculates the optimal threshold by separating these two classes so that their combined intra-class variance is minimized.

Active contour based models are one of the most powerful methods for image segmentation. The basic idea is to evolve a curve around the object which serves as region of interest, toward its interior normal and curve evolution stops on the true boundary of the object subject to the minimization energy. The proposed active contour methods can be classified as Snake model [13] and Level Set model [20]. Snake is an energy minimizing spline guided by the external constraint forces. Level Set method is a shape based tool, which uses a properly defined speed function and it expands or shrinks to acquire any shape of a complex object. In the Level Set method, the initial contour position can be anywhere in the image plane with arbitrary size and does not affect the final segmentation result.

In common practice, there are two categories of level set segmentation techniques, such as: edge based [21], [22] and region based [12], [23], [24] level set segmentation techniques. Edge based methods are sensitive to the initial conditions and have serious boundary leakage problems in images with weak object boundaries. Region based methods give better performance for the images with weak edge boundaries and less affected by noise. Yang [23] proposed a hybrid approach for brain tumor segmentation, which is based on global intensity difference, local edge properties, curve evolution, and level set method. By combining the edge information into the region-based framework, the complex images with intensity irregularities are efficiently segmented. Xie [25] developed a robust region-based active contour

model based on data fitting energy functional using the differences between the local average intensity and the global intensity means. Thapaliya [26] proposed a level set method by developing a signed pressure function (SPF) that can efficiently stop the contours at weak or blurred edges.

Chaplot [27] proposed a classification method using wavelets as input to neural network self-organizing maps and support vector machine for classification of MRI of the human brain. Joshi [28] developed a Neuro Fuzzy Classifier using GLCM to recognize different types of brain tumors.

III. THE PROPOSED METHODOLOGY

Brain tumor imaging analysis is used to extract the patient-specific important clinical information. In this work, a computer aided brain tumor detection scheme is developed with the purpose of enhancing the diagnostic capabilities of physicians and a reduction of the complexity of the accurate diagnosis. The proposed methodology is aimed to develop a computer-aided diagnostic system for the automatic detection of brain tumor through an MRI. The proposed CAD system is shown in Fig. 1.
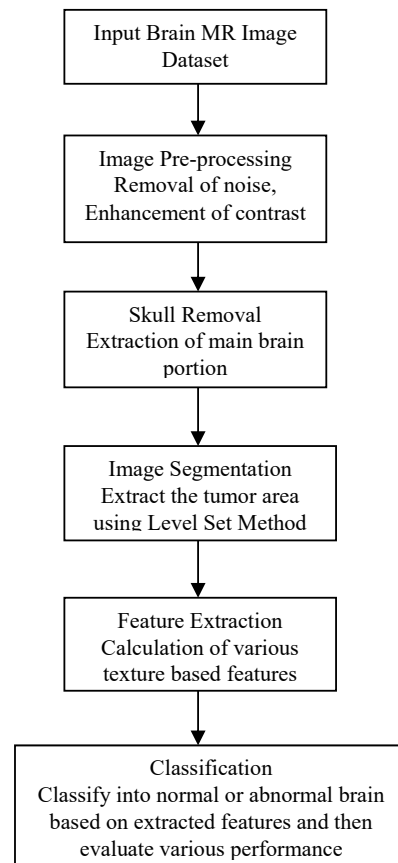
Input Brain MR Image Dataset

↓

Image Pre-processing
Removal of noise, Enhancement of contrast

↓

Skull Removal
Extraction of main brain portion

↓

Image Segmentation
Extract the tumor area using Level Set Method

↓

Feature Extraction
Calculation of various texture based features

↓

Classification
Classify into normal or abnormal brain based on extracted features and then evaluate various performance

Fig. 1 Proposed CAD system for automatic detection of brain tumor

A. Input Brain MR Image Dataset

In this CAD system, the input images are taken as MR images as they provide rich information about the soft tissue anatomy and have drastically improved the quality of brain

pathology, diagnosis and treatment [27]. The input dataset contains 50 abnormal (images contain brain tumor) MR images. The abnormal brain images contain various brain tumor types, such as Glioma, Sarcoma, Meningioma, Metastatic bronchogenic carcinoma, Metastatic adenocarcinoma. The images are axial, T2-weighted, 256 × 256 pixel MR images collected from Harvard Medical School website [29]. The formal interpretation of these images is based on the symmetry property which is observed mostly in axial and coronal images. The normal brain is almost symmetrical in two halves along the mid-line of the axial image. Any notable asymmetry refers to abnormality of the brain [27], and thus, it seems to be an effective feature while considering the image to be normal or abnormal. The normal and abnormal brain images are shown in Fig. 2 (a) and Fig. 2 (b), respectively. But it is not sufficient to classify a brain with tumor. Hence further image processing analysis is preformed to clearly indicate whether the brain is normal or abnormal with certain types of tumor present. While performing these operations on T2WI, it has to be assumed that the edema and brain tumor portion appears as brighter than other normal brain tissues [4].
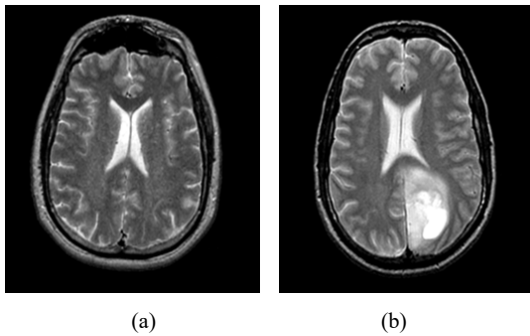

(a)   (b)

Fig. 2 Axial T2-weighted MR brain images: (a) normal brain, (b) abnormal brain (contains glioma tumor)

B. Image Pre-Processing

Image enhancement refers to various types of manipulation on the image matrix, resulting in an optimized output image. An automatic detection requires pre-processed images. Image pre-processing steps make the image segmentation more accurate by removing the common noise and artifacts and adjusting the contrast.

1. Removal of Noise

The noise is introduced while acquiring the image due to various hardware related artifacts, different environmental conditions, patient related motion artifacts because of gross movement of the body during the acquisition period and many others which leads to a degraded MR acquired signal. So the purpose is to eliminate these to a certain extent. While performing various image processing techniques the most common cause of noise encountered is due to intensity inhomogeneity which makes the segmentation process a bit difficult. To overcome this, median filter is used for removal of impulse type (commonly known as salt and pepper noise)

noise. The main advantage of using a median filter is that it preserves the edges while removing noise and gives a smoothed image. It improves the overall quality of the image [3]. The median filtering is a non-linear digital filtering technique

$$I_m(x,y) = median(I(x_n, y_n)) \qquad (1)$$

where $I(x_n, y_n)$, is the input noisy image and $I_m(x,y)$ is the filtered image. The coordinates of the points (x_n, y_n) belong to square neighbourhood of the point (x,y). The basic idea of median filtering is to run through image pixels entry by entry and replacing each pixel entry by the median value of the neighboring pixel entries. The orientation of the neighbors is called the "window" which moves entry by entry throughout the whole image. The median value is calculated by sorting all pixel values from the corresponding neighborhood into an orderly fashion and then replacing the pixel value being considered with the centre pixel value. The median filter of size 3 × 3 is used in this work.

2. Enhancement of Contrast

In medical imaging, contrast is defined as the relative difference between the intensities of two adjacent regions. The factors that influence contrast in MR imaging includes magnetic field strength, magnetic field inhomogeneity, poor illumination and low sensitivity of neuroimaging sensors. While analyzing the brain MR images, it was found difficult to differentiate various tissue regions due to the low contrast of the image. Therefore, the enhancement of contrast is necessary for those types of images. In addition, various image segmentation procedures demand a good contrast enhanced image as input. The contrast of the image is changed by mapping the gray levels in the image to new values through a gray-level transform called contrast stretching. In this proposed method the linear stretching of contrast is used. It is performed by sliding the windows over the entire image and the transformed image is obtained as:

$$g(x,y) = abs[\frac{255}{L_{max}-L_{min}}(f(x,y) - L_{min})] \qquad (2)$$

where $f(x,y)$ is the 8-bit input grayscale image with maximum intensity value of L_{max} and minimum intensity value of L_{min} and $g(x,y)$ is the contrast enhanced image.

C. Removal of Skull and Other Non-Brain Tissue

In this work a fully-automatic segmentation approach is used which successfully separate main brain from non-brain regions. For this purpose, the initial segmentation is carried out using the global thresholding method proposed by Otsu [9]. Let the 2D gray-scale be represented in L number of gray levels $[1,2, \ldots \ldots, L]$. The number of pixels at level i is denoted by n_i and the total number of pixels by $N = n_1 + n_2 + \cdots + n_L$. Then, the normalized probability distribution function is given as:

$$p_i = \frac{n_i}{N} \;\; ; \;\; p_i \geq 0 \; ; \;\; \sum_{i=1}^{L} p_i = 1 \qquad (3)$$

The thresholding method separates the pixels into two classes C_0 and C_1 (background and foreground or object) by a threshold at level K, where C_0 denotes the pixels with levels $[1,2,\ldots,K]$ and C_1 denotes the pixels with levels $[K+1,\ldots\ldots,L]$. Then, the probability of class occurrence and class mean levels are given by:

$$\omega_0 = \Pr(C_0) = \sum_{i=1}^{k} p_i = \omega(k) \qquad (4)$$

$$\omega_1 = \Pr(C_1) = \sum_{i=k+1}^{L} p_i = 1 - \omega(k) \qquad (5)$$

$$\mu_0 = \sum_{i=1}^{k} i\frac{p_i}{\omega_0} = \mu(k)/\omega(k) \qquad (6)$$

$$\mu_1 = \sum_{i=k+1}^{L} \frac{ip_i}{\omega_1} = \frac{\mu_T - \mu(k)}{1 - \omega(k)} \qquad (7)$$

$$\mu(k) = \sum_{i=1}^{k} i\, p_i \qquad (8)$$

μ_T is the total class mean level of the original image. Upon calculation it is observed that total variance is given by:

$$\sigma_T{}^2 = \sum_{i=1}^{L}(i - \mu_T)^2\, p_i \qquad (9)$$

Thus using the threshold value the image is segmented into background and object. The obtained binary image can be expressed as:

$$g_b(x,y) = \begin{cases} 1 & if\ f(x,y) \geq T \\ 0 & otherwise \end{cases} \qquad (10)$$

where $f(x,y)$ is the original intensity value at pixel location (x,y). The segmented image g_b contains the outermost dark region which represents the background, the next white region represents the scalp and the inner dark region represents the skull and CSF, whereas the innermost white region represents the brain.

The objective of this stage of segmentation is to generate a rough brain mask and from there extract the main brain portion. The various steps are discussed below:

- The input original image is taken as 2D grayscale T2-weighted MR image. In T2-weighted MR brain images, the skull appears as darker than brain tissues.
- Then the noise and the intensity in-homogeneities are removed by median filtering process.
- This filtered image is then segmented in two regions namely, foreground (1) and background (0) by a global thresholding method proposed by Otsu [9].
- The whole binary image is labeled using connected component analysis concept. While labeling the adjacent pixels of a neighborhood, the 8-connectivity of neighborhood is considered. Thus, the whole binary image is converted into a labeled binary image.
- Then the brain region is selected from these connected components according to some prior information. The area of each connected regions is calculated. For each image, the largest area of the connected component among the regions obtained is taken as the main brain

portion. The other components are redundant and are not taken into consideration. Thus, this step generates a rough brain mask.

D. Segmentation of Brain Tumor Using Level Set Method

Segmentation is an important image processing technique to extract the region of interest from a complex MR brain image. Active contour based models are one of the most powerful methods for image segmentation. The basic idea is to evolve a curve around the object which serves as region of interest, toward its interior normal and curve evolution stops on the true boundary of the object subject to the minimization energy. In the level set method, the interface is represented implicitly by the zero level set of a function, $\emptyset(x) = 0$, where $\emptyset$ is defined for all x, not just the ones on the boundary. To represent $\emptyset$ in a finite form on a computer a discretized mesh grid is used.

The Zero Level Set of an implicit function $\emptyset$ defined over the entire image I. This function changes with time according to the speed function F. The Curve C is represented implicitly by a Lipschitz function $\emptyset$ as, $C = \{ (x,y)|\emptyset(x,y) = 0\}$ and the evolution of curve is given by the zero-level set curve $\emptyset(t,x,y)$, at time t. The curve is evolved in normal direction with speed term F. The evolution of $\emptyset$ [20] is defined by partial differential equation in (11).

$$\frac{\partial\emptyset}{\partial t} = |\nabla\emptyset|\, F = |\nabla\emptyset|div\left(\frac{\nabla\emptyset}{|\nabla\emptyset|}\right) \qquad (11)$$

$$\emptyset(0,x,y) = \emptyset_0(x,y), t \in (0,\infty),\ x \in R^2 \qquad (12)$$

The set $\{(x,y)|\emptyset_0(x,y) = 0\}$ defines the initial contour. On the interior of $C, \emptyset > 0$ and on the exterior of $C, \emptyset < 0$.

The simplified Chan-Vese [24] energy minimization model is used in this work. Let Ω be the image domain of gray level image I. Then the energy function to be minimized can be expressed as:

$$E(c_1,c_2,C) = \mu.length(C) + \lambda_1 \int_{inside(C)} |I(x) - c_1|^2 + \lambda_2 \int_{outside(C)} |I(x) - c_2|^2\ ,\ x \in \Omega \qquad (13)$$

where outside (C) and inside (C) represent the regions outside and inside the curve C, respectively, c_1 and c_2 designate two constants that approximate the image intensities in outside (C) and inside (C), respectively. λ_1 and λ_2 are fixed constants. The third term is the length of curve C for regularization. Typically $\lambda_1 > 0, \lambda_2 > 0$ and $\mu \geq 0$.

The values c_1 and c_2 can be obtained by minimizing the energy term and obtained as:

$$c_1(\emptyset) = \frac{\int_\Omega I(x).H(\emptyset)dx}{\int_\Omega H(\emptyset)dx} \qquad (14)$$

$$c_2(\emptyset) = \frac{\int_\Omega I(x).(1-H(\emptyset))dx}{\int_\Omega (1-H(\emptyset))dx} \qquad (15)$$

where $H(\emptyset)$ is the Heaviside function and the one-dimensional Dirac measure ∂_0 are defined as:

$$H(\emptyset) = \begin{cases} 1, & if \; \emptyset \geq 0 \\ 0, & if \emptyset < 0 \end{cases}, \; \partial_0(\emptyset) = \frac{d}{d\emptyset}H(\emptyset) \qquad (16)$$

Heaviside function $H(\emptyset)$ is replaced with a smooth function that approximates $H(\emptyset)$ called the smoothed Heaviside function and gives a global minimum of energy and is defined as:

$$H_\varepsilon(\emptyset) = \frac{1}{2}[1 + \arctan(\frac{x}{\varepsilon})], \; \text{for} \; -\varepsilon < \emptyset < \varepsilon \qquad (17)$$

and its derivative that is the Dirac delta function is given as:

$$\partial_\varepsilon(x) = H_\varepsilon{}'(x) = \frac{1}{\pi} \cdot \frac{\varepsilon}{\varepsilon^2 + x^2} \qquad (18)$$

after evolving $\emptyset$ under a general speed function F, it generally does not remain a signed distance function. So $\emptyset$ is reinitialized [30] by finding a new $\emptyset$ with the same zero level set but with $|\nabla\emptyset| = 1$. Thus

$$\frac{\partial\emptyset}{\partial t} + sign(\emptyset)(|\nabla\emptyset| - 1) = 0 \qquad (19)$$

E. Texture Feature Extraction Using GLCM

The next process after image segmentation is the extraction of texture features from the segmented image which is found to be very helpful for proper analysis of an image in a large scale. Texture is considered as a surface property of every object and each object has its own statistical textural feature, so it differs from each other.
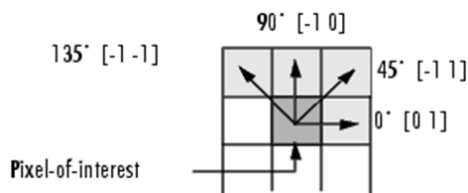

Fig. 3 Orientation and directionality used to calculate GLCM with distance d=1

Haralick [31] first introduced the use of co-occurrence probabilities using GLCM for extracting various texture features. The GLCM is a two dimensional histogram of gray levels for a pair of pixels, which are separated by a fixed spatial relationship. GLCM of an image is computed using a displacement vector defined by its radius d and orientation θ. In this work, the four angular orientations are taken as 0°, 45°, 90° and 135°. The separation distance d is taken as unity. Their relationship is shown in Fig. 3.

The textural properties are derived using: a) first-order statistics and b) second-order statistics that are computed from gray-level co-occurrence matrices (GLCMs). The normalized feature vectors are computed by normalizing the probability of occurrence over the window size of a 3×3 pixel matrix. The feature vector includes three features derived from first-order statistics such as: (i) mean, (ii) standard deviation, and (iii) entropy; and from second-order statistics: (i) contrast, (ii) angular second moment, (iii) inverse difference moment, (iv) autocorrelation, (v) homogeneity, (vi) variance, (vii) cluster shade, (viii) sum average, (ix) inertia, (x) cluster prominence and (xi) dissimilarity [31].

An algorithmic approach which is used in this work for the calculation of GLCM based texture features is given as:

– Take input images as 2D grayscale 8-bit images with dimension 256×256.
– Quantize the image to a desired level (here in this work 256 quantization level is used).
– Select a proper window of M×N, the distance value d and the various orientation angles θ. In this work a 3×3 resolution window with separation distance of unity is taken. The four angles are taken as 0°, 45°, 90° and 135°.
– Calculate the GLCM matrix by constructing a frequency table for each gray-level pair occurrence. Repeat this step for each angle orientation of θ. So there will be four GLCM matrices for this work.
– To obtain a symmetrical GLCM matrix add it to the transpose of the GLCM matrix.
– Normalize each GLCM matrix by dividing each element of the matrix by the sum of all elements present in that matrix. This may serve as conditional probability matrix.
– Calculate each of the features described earlier for each of the four GLCM matrices.
– For each feature, the angular mean is calculated by taking the simple mean of those features obtained from four GLCM matrices.

F. Classification of Brain MR Images Using Feed Forward Back Propagation Neural Network

After extracting the valuable textural features, the brain tumor MR images are classified into their respective types. For this classification, a feed forward back propagation neural network is taken into account. ANNs are interconnected networks used to perform a specific computational task. A specific input node is viewed as the weighted sum of the all possible combination of nodes to which it is interconnected. In this proposed method one input layer, one hidden layer and one output layer is taken. The input layer contains 16 nodes, the hidden layer contains 10 nodes and the output layer contains five nodes. The corresponding model is shown in Fig. 4.
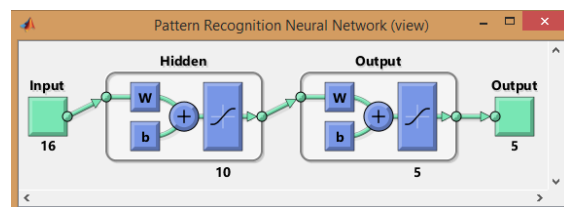

Fig. 4 The neural network model for classification of 5 types of brain tumor

W is the weight variable and b is the bias parameter. The activation transfer function used for hidden and output layer is of log-sigmoid type which is given as:

$$logsig(n) = 1 / (1 + exp(-n)) \qquad (20)$$

The function generates outputs between 0 and 1 as the neuron's net input goes from negative to positive infinity.

The network is trained using scaled conjugate gradient back propagation algorithm [32]. It is fully automatic supervised learning algorithm and has a fast convergence rate.

The output of the neural network is described by:

$$y = F_o(\sum_{j=0}^{M} W_{oj}(F_h(\sum_{i=0}^{N} W_{ji} x_i))) \qquad (21)$$

where W_{oj} represents the synaptic weights from neurons in the hidden layer to the single output neuron, x_i represents the i-th element of the input vector, F_h and F_o are the activation function of the neurons from the hidden layer and output layer, respectively, W_{ji} are the connection weights between the neurons of the hidden layer and the inputs [3].

The learning phase of the network proceeds by adaptively adjusting the free parameters of the system based on the mean square error E:

$$E = \frac{1}{2}\sum_{i=1}^{n}(y_i - d_i)^2 \qquad (22)$$

where the output value, y_i is calculated by the network and d_i represents the expected output. When the error between network output and the desired output is minimized, the learning process is terminated and the network can be used in a testing phase with test vectors. Then the neural network is described by the optimal weight configuration, which theoretically ensures the output error minimization [3].

IV. RESULTS AND DISCUSSION

The images are taken from Harvard Medical School database [29]. The original images collected from Harvard Medical School database contain some amount of noise. This noise is removed using a median filter. The noise removed and smoothed images are shown in Fig. 5.
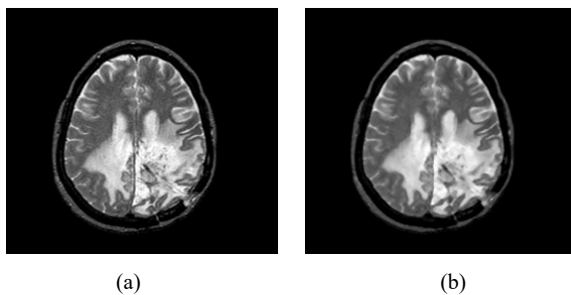

(a)   (b)

Fig. 5 Images before (a) and after (b) median filter is applied

The original database images contains the brain with skull and other non-brain parts such as scalp, skin, eyeballs etc. These portions of the image are removed using several image processing steps. The input image is taken as median filtered original image. At first, the gray-scale image is thresholded by a global thresholding technique proposed by Otsu. Then these binary images are labeled using run length identification scheme and different connected components are computed considering 8-neighborhood connectivity. The areas of each of these connected components are calculated. Among these the largest connected component area is considered which serves as rough brain mask. Using this binary mask the original 2D gray-scale extracted brain portion is computed. The original images and their corresponding brain parts are shown in Fig. 6.

(a)   (b)

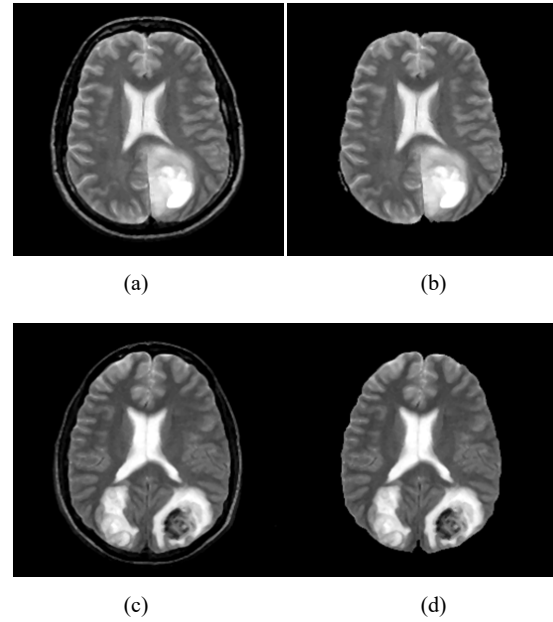(c)   (d)

Fig. 6 Original filtered images (a), (c) and their corresponding skull removed (b), (d) segmented brain MR images

After removing the skull and other non-brain parts, the brain image is then segmented to extract the tumor part. In this work different types of brain tumor images are segmented using a Level Set based method. At first, an initial contour is taken as a rectangular shaped image which covers the region of interest, in this case the brain tumor portions. Then after a certain number of iterations are performed, it gives the rough segmented binary image. Then these binary tumor portion images are applied to original images to get the actual gray-scale tumor portion. The results of the segmentation process and the final segmented tumors output are shown in Fig. 7.

(a)   (b)   (c)

(d)   (e)   (f)

(g)   (h)   (i)

Before Segmentation   After Segmentation   Final Segmented
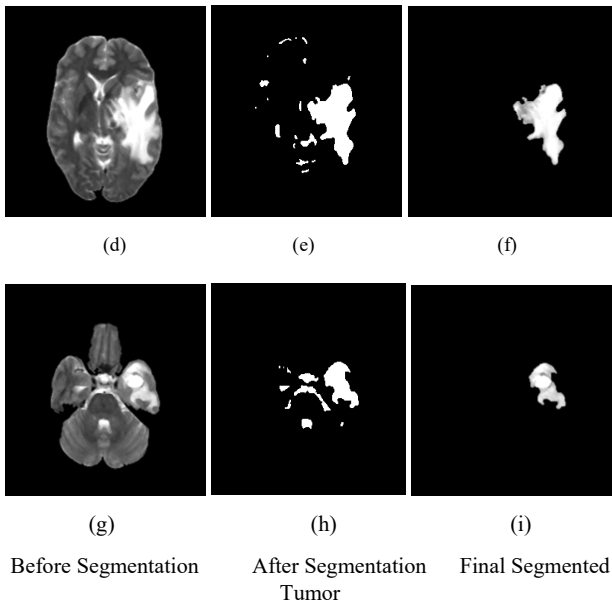   Tumor
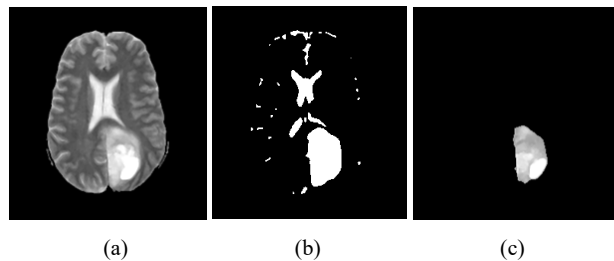
Fig. 7 Level set segmentation of different types of brain tumor MR images: original skull-removed median filtered images (a), (d), (g) corresponding segmented binary images (b), (e), (h) Segmented tumor (c), (f), (i)
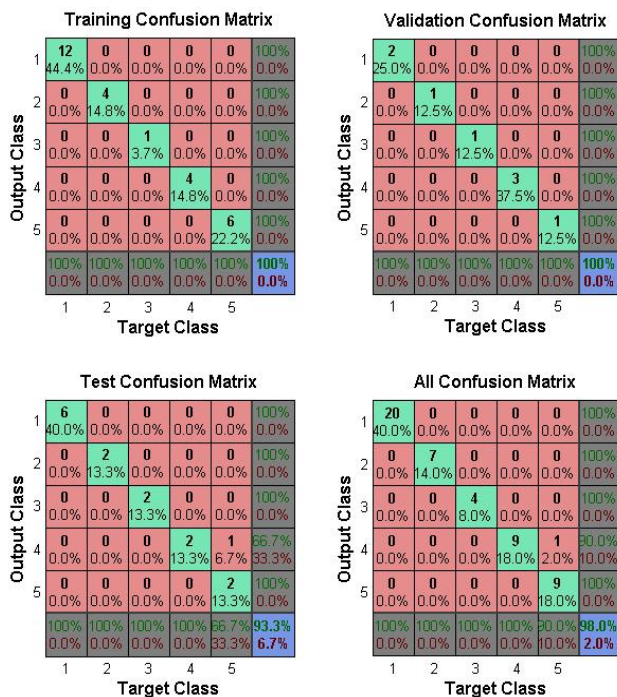

Fig. 8 ANN confusion matrix for classification of five types of brain tumor patients

The texture features are calculated from the GLCM in this work. The texture features considered in this work are: autocorrelation, contrast, correlation, dissimilarity, energy, entropy, homogeneity, maximum probability, variance, sum average, sum variance, sum entropy, difference entropy, cluster prominence, and cluster shade.

The feature set contains 16 texture features of 20 Glioma, seven Meningioma, four Metastatic Adenocarcinoma, nine Metastatic Bronchogenic Carcinoma and 10 Sarcoma type of segmented brain tumor MR images considered for classification. The extracted features of the segmented brain tumor images obtained from the Level Set based segmentation are given as the input data matrix to the neural network. Thus, there will be five classes, and are labeled as class 1 to class 5, respectively. The network is trained by scaled conjugate backpropagation technique. The overall classification accuracy obtained using this method is 98%. The confusion matrix obtained is shown in Fig. 8.

V. Conclusion

Many of the current segmentation techniques are operated on MR images due to its excellent soft-tissue contrast. The purpose of these methods is to assist the physicians to take a preliminary decision on diagnosis, monitoring, and therapy planning for the patients having brain tumor. The semi-automatic and fully automatic segmentation of a brain tumor from abnormal brain images experiences great challenges due to irregularities in boundaries with discontinuities and partial-volume effects of brain tumor images. The proposed level set segmentation technique gives better performance over the images with weak edge boundaries, less sensitive to the initial position of the contours, and is less affected by noise as compared to other segmentation methods. It is observed that the proposed methodology performs complete segmentation of the brain portion from non-brain tissues, skull and more importantly the tumor part. It requires only minimal manual selection of some parameters. Intra-observer variability, which is often introduced in manual segmentation process, is significantly reduced with the help of this automated method. Besides, due to the high amount of scans to be visualized, expert's fatigue, and the complexity of images, it is observed that some small brain tumor portions are being missed without using a computer-aided tool. Hence, there is a risk of a patient being not diagnosed properly. The utilization of a CAD tool would serve to improve not only the efficiency, but also, the accuracy of brain tumor screening performed on cancer patients. The segmentation and classification accuracy with this automated method is very high. Thus, the proposed system will definitely reduce the false positive and false negative rate and cancer patients will be diagnosed in a more accurate way.

References

[1] The Essential Guide to Brain Tumors, National Brain Tumor Society, http://www.braintumor.org

[2] A. Drevelegas (ed.), "Imaging of Brain Tumors with Histological Correlations," Springer-Verlag Berlin Heidelberg 2011.

[3] El-Sayed A. El-Dahshan et al. "Computer-Aided Diagnosis of Human Brain Tumor through MRI: A Survey and a New Algorithm," *Expert Systems with Applications*, 41 (2014), 5526–5545.

[4] Jainy Sachdeva et al. "A Novel Content-Based Active Contour Model for Brain Tumor Segmentation," *Magnetic Resonance Imaging*, 30 (2012), 694–715.

[5] Stephen M. Smith, "Fast Robust Automated Brain Extraction," *Human Brain Mapping*, 17:143–155(2002).

[6] K. Somasundaram, T. Kalaiselvi, "Automatic Brain Extraction Methods for T1 Magnetic Resonance Images Using Region Labeling and Morphological Operations," *Computers in Biology and Medicine*, 41 (2011), 716–725.

[7] Jiang et al. "Brain Extraction from Cerebral MRI Volume using a Hybrid Level Set Based Active Contour Neighborhood Model," BioMedical Engineering OnLine 2013, 12:31, http://www.biomedical-engineering-online.com/content/12/1/31

[8] Gordillo N et al. "State of the Art Survey on MRI Brain Tumor Segmentation," *Magnetic Resonance Imaging*, 31 (2013), 1426–1438.

[9] Nobuyuki Otsu, "A Threshold Selection Method from Gray-Level Histograms," *IEEE Transactions on Systems, Man, and Cybernetics*, VOL. SMC-9, NO.1, January 1979.

[10] Dubey et al. "Region Growing for MRI Brain Tumor Volume Analysis," *Indian Journal of Science and Technology,* Vol.2 No. 9 (Sep 2009).

[11] Jafari, M, Kasaei, S, "Automatic Brain Tissue Detection in MRI Images Using Seeded Region Growing Segmentation and Neural Network Classification," *Australian Journal of Basic and Applied Sciences*, 5(8), 1066–1079.

[12] Chunming Li et al. "A Level Set Method for Image Segmentation in the Presence of Intensity Inhomogeneities with Application to MRI," *IEEE Transactions on Image Processing*, VOL. 20, NO. 7, JULY 2011.

[13] Michael Kass et al. "Snakes: Active contour models," *International Journal of Computer Vision*, Volume 1, Issue 4, pp 321-331, January 1988.

[14] Matthew C. Clark et al. "Automatic Tumor Segmentation Using Knowledge-Based Techniques," *IEEE Transactions on Medical Imaging*, Vol. 17, No. 2, April 1998.

[15] Gudrun Wagenknecht et al. "Knowledge-based Segmentation of Attenuation-relevant Regions of the Head in T1-weighted MR Images for Attenuation Correction in MR/PET Systems," *IEEE Nuclear Science Symposium Conference Record*, M09-287, 2009.

[16] Nara M. Portela et al. "Semi-Supervised Clustering for MR Brain Image Segmentation," *Expert Systems with Applications*, 41 (2014) 1492–1497.

[17] Sanjay Agrawal et al. "A Study on Fuzzy Clustering for Magnetic Resonance Brain Image Segmentation Using Soft Computing Approaches," *Applied Soft Computing*, 24(2014), 522–533.

[18] D.Jude hemanthl et al. "Effective Fuzzy Clustering Algorithm for Abnormal MR Brain Image Segmentation," *IEEE International Advance Computing Conference (IACC 2009)*, Patiala, India, 6-7 March 2009.

[19] P. Moallem et al. "Optimal Threshold Computing in Automatic Image Thresholding using Adaptive Particle Swarm Optimization," http://www.researchgate.net/publication/233814424

[20] Osher, S., and Sethian J.A., "Fronts Propagating with Curvature Dependent Speed: Algorithms Based on Hamilton-Jacobi Formulations," Journal of Computational Physics, 79, pp.12-49, (1988).

[21] Vicent Caselles et al. "Geodesic Active Contours," International Journal of Computer Vision, 22(1), 61–79 (1997).

[22] O. Michailovich, Y. Rathi, A. Tannenbaum, "Image Segmentation Using Active Contours Driven by the Bhattacharyya Gradient flow," IEEE Trans. Image Process. 15 (11) (2007) 2787–2801.

[23] Hongzhe Yang et al. "Brain Tumor Segmentation Using Geodesic Region-based Level Set without Re-initialization," International Journal of Signal Processing, Image Processing and Pattern Recognition, Vol.7, No.1 (2014), pp.213-224.

[24] Tony F. Chan, Luminita A. Vese, "Active Contours Without Edges," IEEE Transactions on Image Processing, Vol. 10, No. 2, February 2001.

[25] Xiaomin Xie et al. "A Robust Level Set Method Based on Local Statistical Information for Noisy Image Segmentation," Optik 125 (2014) 2199–2204, http://dx.doi.org/10.1016/j.ijleo.2013.10.026

[26] Kiran Thapaliya et al. "Level Set Method with Automatic Selective Local Statistics for Brain Tumor Segmentation in MR Images," Computerized Medical Imaging and Graphics, 37 (2013) 522– 537.

[27] Sandeep Chaplot et al. "Classification of Magnetic Resonance Brain Images Using Wavelets as Input to Support Vector Machine and Neural Network," Biomedical Signal Processing and Control, 1 (2006) 86–92.

[28] Dipali M. Joshi et al. "Classification of Brain Cancer Using Artificial Neural Network," 2nd International Conference on Electronic Computer Technology (ICECT 2010).

[29] http://med.harvard.edu/ANNALIB

[30] Mark Sussman et al. "A Level Set Approach for Computing Solutions to Incompressible Two Phase Flow," Journal of Computational Physics, 114, 146-159, (1994).

[31] Harlick et al. "Textural Features for Image Classification", IEEE Transactions on Systems, Man and Cybernetics, Vol. SMC-3, No-6, November 1973, pp. 610-621.

[32] Martin Fodslette Moller, "Scaled Conjugate Gradient Algorithm for Fast Supervised Learning," Neural Networks, Vol. 6, pp. 525-533, 1993.